

# Signatures of Spin Degrees of Freedom in Charge Dynamics of $\text{YBa}_2\text{Cu}_3\text{O}_{6.95}$

E. Schachinger<sup>a</sup> and J.P. Carbotte<sup>b</sup>

<sup>a</sup>Institut für Theoretische Physik, Technische Universität Graz, A-8010 Graz, Austria

<sup>b</sup>Department of Physics and Astronomy, McMaster University, Hamilton, Ont. L8S 4M1, Canada

Charge carrier-spin excitation spectral densities constructed from optical data and varying with temperature are used to calculate various properties of the charge carrier dynamics. Temperature ( $T$ ) variations of such properties are sensitive to the changes in the spectral density brought about by the growth in the 41 meV spin resonance as  $T$  is lowered. The microwave conductivity and the thermal conductivity are stressed and comparison with experiment is given. The imaginary part of the conductivity as a function of frequency  $\omega$  is also featured.

Following the demonstration by Carbotte *et al.* [1] that infrared optical conductivity data could be used to identify the strength and form of the coupling between the charge carriers and the spin degrees of freedom in optimally doped  $\text{YBa}_2\text{Cu}_3\text{O}_{6.95}$  (YBCO), Schachinger and Carbotte [2] extended the analysis to other high  $T_c$  materials. They found that the existence of a spin resonance and its coupling to the charge carriers is not limited to the bilayered materials although it does not exist in all high  $T_c$  superconductors. The essence of the analysis whereby a spectral density is obtained, involves a second derivative of the optical scattering rate. This was first introduced by Marsiglio *et al.* [3] for the electron-phonon case in the normal state, and applied with considerable success to the case of  $\text{K}_3\text{C}_{60}$ , a narrow band system in which correlation effects are expected to be significant. The method was generalized by Carbotte *et al.* [1] to the superconducting state with  $d$ -wave order parameter. This involves generalized Eliashberg equations in which the dominant coupling is assumed to be due to the spins as in the nearly antiferromagnetic Fermi liquid theory by Pines and coworkers [4,5]. The interactions enter only through the carrier-spin spectral function  $I^2\chi(\omega)$ . Further work by Schachinger *et al.* [6] showed that optical data at various temperatures could be used to obtain a spectral density at each temperature and that

these functions reflect the growth of the 41 meV spin resonance measured by inelastic spin polarized neutron scattering [7]. A temperature dependence to the effective spectral density  $I^2\chi(\omega)$  is different from the case of the electron-phonon interaction where there is no significant  $T$  dependence. It is characteristic of highly correlated electron systems in which the effective interaction responsible for superconductivity resides in the electron system itself and therefore is modified by any change in the state of the charge carriers. Spin fluctuations in the nearly antiferromagnetic Fermi liquid model are an example of such a mechanism but is not unique.

In the work of Schachinger *et al.* [6] the temperature dependence of the spectral weight under the 41 meV resonance which contributes to the pairing interaction agrees well with the neutron data Dai *et al.* [7] on the growth of the resonance peak as  $T$  is lowered in the superconducting state. The resulting spectra  $I^2\chi(\omega)$  lead to good agreement with experiment for the temperature dependence of the in-plane superfluid density as well as for the large peak observed well below  $T_c$  in the microwave conductivity. This peak reflects the collapse of the inelastic scattering rate in the superconducting state due to the gapping of the low energy part of the spectral density by the onset of superconductivity. The calculations also offer an explanation for the large value of the gap to

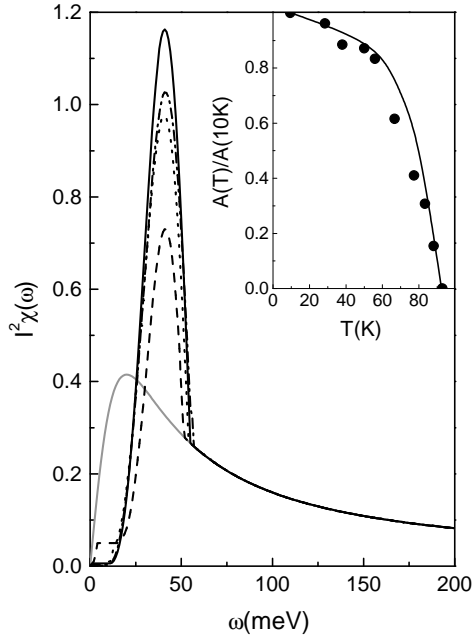


Figure 1. The charge carrier-spin excitation spectral density  $I^2\chi(\omega)$  determined from optical scattering rate data at various temperatures. Gray curve  $T = 95$  K, dashed  $T = 80$  K, dotted  $T = 60$  K, dash-dotted  $T = 40$  K, and solid  $T = 10$  K. Note the growth of the strength of the 41 meV spin resonance as the temperature is lowered. The insert gives the spectral weight under the resonance  $A(T)$  normalized to its  $T = 10$  K value (solid curve) compared with the neutron data of Dai *et al.* [7] for the equivalent quantity (solid circles).

critical temperature ratio observed as compared to the BCS  $d$ -wave value. They give the correct zero temperature condensation energy per copper atom and they predict correctly that the superfluid density is only about 25% of the total optical oscillator strength. This arises because only the coherent quasiparticle part of the electronic spectral function condenses into the superfluid. The large incoherent background remains largely unaffected.

Here we extend the work to include the temperature dependence of the thermal conductivity and

discuss in some detail the fit obtained to optical conductivity data with emphasis on the signature of the spin resonance in this quantity.

In Fig. 1 we show the charge carrier-spin excitation spectral density  $I^2\chi(\omega)$  obtained in the work of Schachinger *et al.* [6] at various temperatures, namely  $T = 95$  K (gray),  $T = 80$  K (dashed),  $T = 60$  K (dotted),  $T = 40$  K (dash-dotted), and  $T = 10$  K (solid). These are constructed by fitting a spin fluctuation form for the effective charge carrier-spin excitation spectral density  $I^2\chi(\omega)$  to optical data via generalized  $d$ -wave Eliashberg equations. First a two parameter form (MMP [4]) is fit to the normal state at  $T = 95$  K,  $I^2\chi(\omega) = I^2\omega/(\omega^2 + \omega_{SF}^2)$ , where  $I$  is a measure of the charge-spin coupling and  $\omega_{SF}$  is an energy characteristic of the spin fluctuations. The fit to the  $T = 95$  K optical scattering rate,  $\tau^{-1}(\omega)$ , determines both parameters.  $I^2$  is adjusted to get the measured magnitude of  $\tau^{-1}(\omega)$  and  $\omega_{SF}$  to reproduce its observed frequency dependence. As the temperature is lowered into the superconducting state the optical data shows the growth of a new collective mode at 41 meV in YBCO. The second derivative of  $\omega\tau^{-1}(\omega)$  with respect to  $\omega$  gives a first estimate of the position, shape, and size of this contribution to the spectral density which is then used to modify  $I^2\chi(\omega)$  in this energy range. Other frequency regions are left unaltered. The curves for  $I^2\chi(\omega)$  change very significantly with  $T$  (see Fig. 1). Also, as shown in the inset of Fig. 1, the spectral weight under the resonant peak agrees well with the spin polarized neutron scattering data of Dai *et al.* [7] for the equivalent quantity.

Once the spectral density of Fig. 1 is known at a particular temperature, the  $d$ -wave Eliashberg equations can be solved for the frequency dependent gap and renormalization function and various properties can be determined from them. As a first result we show in Fig. 2 the temperature dependence of the microwave peak at  $\omega = 0.144$  meV [6]. The solid squares are the experimental data of Bonn *et al.* [8]. The solid circles are our theoretical results assuming a clean sample, i.e. no impurity scattering. We see that there is good agreement at higher temperatures but that the theoretical curve is not broad enough

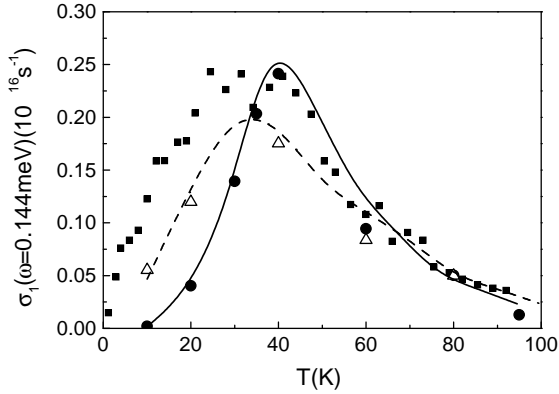


Figure 2. The microwave conductivity at 0.144 meV as a function of temperature  $T$ . The solid squares are the data of Bonn *et al.* [8], the solid circles our theoretical results for the pure case, while the open triangles include some impurity scattering  $\tau_{imp}^{-1} \simeq 1.8$  meV. The solid and dashed curves are guides to the eye.

as  $T$  is reduced. Much better agreement results when a small amount of impurity scattering is included with  $\tau_{imp}^{-1} \simeq 1.8$  meV (open triangles). The solid and dashed curves are from previous work [9] based on a phenomenological spectral density but can also be considered as guides to the eye.

A second quantity of interest is the temperature dependent electronic thermal conductivity  $\kappa_{ab,e}(T)$  (in-plane). This is shown in Fig. 3. The solid squares are the experimental results of Matsukawa *et al.* [10] and the open triangles are our numerical results. We see that the agreement is good and that our spectral densities are capable of describing the observed transport properties of optimally doped YBCO.

In the procedure followed to obtain the  $I^2\chi(\omega)$  of Fig. 1 only the optical scattering rate  $\tau^{-1}(T, \omega) = \Omega_p^2 \{\text{Re}[\sigma^{-1}(T, \omega)]\} / 4\pi$  is used. Here  $\sigma(T, \omega)$  is the infrared a.c. conductivity as a function of frequency  $\omega$ , at temperature  $T$ , and  $\Omega_p^2$  is the plasma frequency obtained from the in-plane optical oscillator strength. In Fig. 4 we show our theoretical results for  $\omega$  times the imaginary part of the optical conductivity,  $\omega\sigma_2(\omega)$ , as a func-

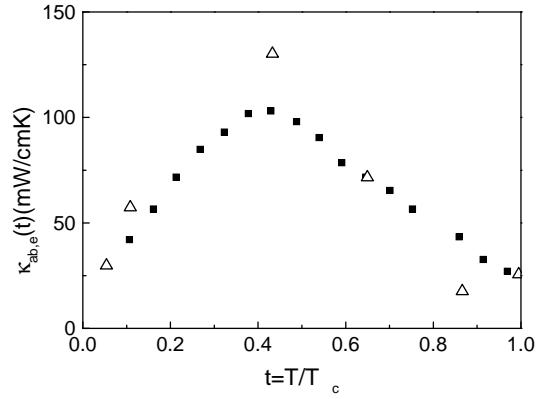


Figure 3. The electronic part of the thermal conductivity as a function of temperature  $T$ . The solid squares are the experimental results of Matsukawa *et al.* [10] and the open triangles our theoretical result.

tion of  $\omega$  at  $T = 10$  K and compare with data of Homes *et al.* [11] (solid curve). Several points can be made. First, as shown by Schachinger *et al.* [6] the limit  $\omega \rightarrow 0$  of  $\omega\sigma_2(\omega)$  fits well the measured temperature dependence of the superfluid density. Second, the dotted curve which is included for comparison was obtained using the normal state MMP [4] spectrum and does not include the 41 meV resonance. The other two curves in Fig. 4 (dashed, pure case, dash-dotted with some impurities) do and this has improved the agreement with the data substantially. The minimum at  $\omega = 75$  to 80 meV (equal to approximately twice the gap plus the resonance frequency  $\omega_{sr}$ ) can be traced to the resonance peak and is its signature. No such minimum would exist in a BCS formulation of  $d$ -wave superconductivity.

In Fig. 5 we show results for the real part of  $\sigma(T, \omega)$  at  $T = 10$  K. The solid gray curve is BCS and shows no agreement with experimental data (black curve). It is clear that the high  $T_c$  superconductors are far from simple BCS superconductors modified to account for the  $d$ -wave symmetry of the gap. The dotted curve gives results of Eliashberg calculations based on the solid gray curve of Fig. 1 for  $I^2\chi(\omega)$  which does not include effects of the 41 meV spin resonance. This curve is

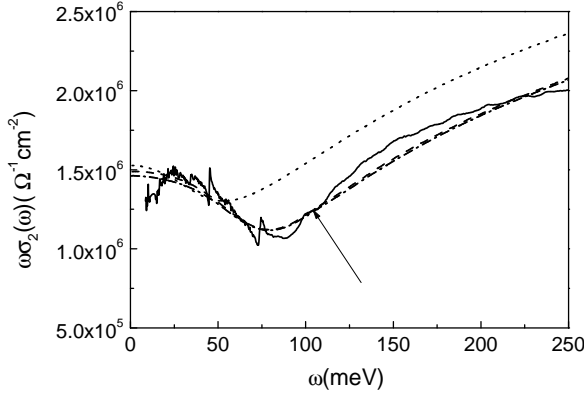


Figure 4. The imaginary part of the optical conductivity,  $\sigma_2(\omega)$ , times  $\omega$  as a function of  $\omega$ . The solid black curve is the data [11], the dotted curve theoretical results based on the MMP spectral density with  $\omega_{SF} = 20$  meV without modification for the 41 meV resonance peak while the dashed and dash-dotted curve include it. Dashed is for the pure case, dash-dotted includes elastic impurity scattering with  $\tau_{imp}^{-1} \simeq 1.8$  meV. The arrow indicates the data point used to fit theory to experiment.

important for comparison with results of a calculation which includes the resonance, dashed curve in the clean limit and dash-dotted curve with a small amount of elastic impurity scattering. Including the 41 meV resonance in the spectral density has improved agreement with experiment by shifting the main rise in the conductivity (after the remaining Drude like part at very small  $\omega$  has largely died out) to higher energies.

In conclusion, the formation of the 41 meV spin resonance in the superconducting state of optimally doped YBCO can be tracked accurately through the optical conductivity which carries a signature of its growth with decreasing temperature. The resonance plays an important role in the transport and thermodynamic properties of YBCO leading to distinct temperature dependences and characteristic structure in spectroscopic quantities as a function of frequency  $\omega$ .

Research supported in part by NSERC (Natural Sciences and Engineering Research Council

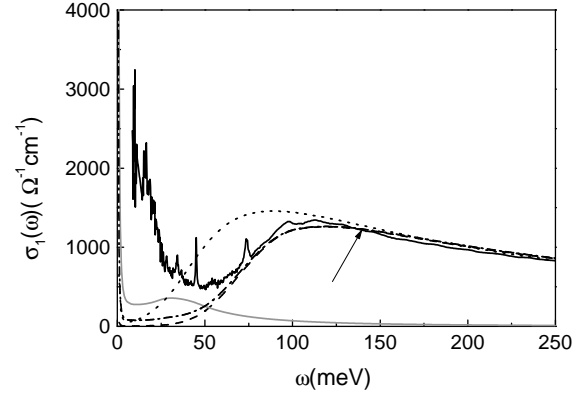


Figure 5. The real part,  $\sigma_1(\omega)$ , of the optical conductivity with various curves the same as in Fig. 4. The additional solid gray curve is the result of a BCS  $d$ -wave calculation.

of Canada) and by CIAR (Canadian Institute for Advanced Research). The authors are grateful to Dr. D.N. Basov and Dr. C.C. Homes for supplying their original experimental data.

## REFERENCES

1. J.P. Carbotte, E. Schachinger, and D.N. Basov, *Nature* 401 (1999) 354.
2. E. Schachinger and J.P. Carbotte, *Phys. Rev. B* 62 (2000) 9054.
3. F. Marsiglio, T. Startseva, and J.P. Carbotte, *Physics Lett. A* 245 (1998) 172.
4. A.J. Millis, H. Monien, and D. Pines, *Phys. Rev. B* 42 (1990) 167.
5. P. Monthoux and D. Pines, *Phys. Rev. B* 47 (1993) 6064.
6. E. Schachinger, J.P. Carbotte, and D.N. Basov, *Europhysics Letters* (submitted).
7. P. Dai *et al.*, *Science* 284 (1999) 1344.
8. D.A. Bonn *et al.*, *Phys. Rev. B* 47 (1993) 11314.
9. E. Schachinger, J.P. Carbotte, and F. Marsiglio, *Phys. Rev. B* 56 (1997) 2738.
10. M. Matsukawa *et al.*, *Phys. Rev. B* 53 (1996) R6034.
11. C.C. Homes *et al.*, *Phys. Rev. B* 60 (1999) 9782.